JOURNAL OF MATERIALS SCIENCE 22 (1987) 761–769

Review
Ionic conduction and conduction polarization in oxide glass

AKIRA DOI
Department of Materials, Nagoya Institute of Technology, Nagoya 466, Japan

Biasing of an oxide glass by an applied electric field is reviewed with emphasis on the present author's works on thermally stimulated polarization/depolarization current and its relationship with d.c./a.c. conduction and dielectric relaxation. Evidence is presented supporting the idea that in oxide glass conduction should be accompanied by polarization, termed conduction polarization.

1. Introduction

The results of biasing of an oxide glass by an applied electric field, based principally on the present author's works on thermally stimulated polarization/depolarization current (TSPC/TSDC) [1–14] are reviewed here. The term "to bias" means to give an electrical potential difference or a difference in the free-electron density on both sides of the sample using an electron pump as battery or d.c./a.c. power supply. For this purpose, both sides of the sample are provided with electron-conductive materials as evaporated metals, metal plates or conductive pastes which act as the electrodes.

Various techniques are known but we shall restrict ourselves to those which derive information *in situ* from the electrodes, i.e. those of d.c./a.c. conduction, dielectric relaxation, and TSPC/TSDC. The d.c. conduction method measures a current which flows in the external circuit when a sample is biased by d.c. electric field as a function of time. Initially we observe a transient (termed the absorption current) then a steady current (the leakage current) and, at longer times, a current decay due to the space-charge effect (Fig. 1) [15]. The absorption current is believed to be due to dielectric relaxation, and the leakage current to be due to electrical conduction, because the latter fits well with a theoretical description for d.c. conductivity

$$\sigma_{d.c.} = \sigma_0 \exp(-H/kT) \quad (1)$$

where σ_0 is the pre-exponential factor and H the activation energy for conduction. The a.c. conduction method is an alternative to its d.c. counterpart utilizing an a.c. rather than d.c. applied field for the purpose of reducing the space-charge effect which frequently is encountered and is a nuisance to d.c. measurements.

Dielectric measurement is a procedure for obtaining information about polarization, i.e. about distorted distribution of the charge carriers within a sample. When the sample is biased by an a.c. field, the charge carriers move in response to a change of the applied field, and so would move in response the total number of electrons on the electrode which are composed of free electrons (to give the bias voltage) and bound electrons (to be induced by polarization). We can determine how the relevant charge carriers respond to a change of the applied field by measuring the dielectric constant

$$\varepsilon = D/E \quad (2)$$

as a function of frequency, where E is the applied field and D the displacement which is defined as the apparent field caused by total electrons accumulated on the electrode. When a frequency is reduced gradually from infinity, a frequency f_m is reached at which relevant charge carriers can follow the change of E with time, hence ε increases by $\Delta\varepsilon$ (Fig. 2). Such an increase in ε is termed the dielectric dispersion or relaxation. Almost all glasses exhibit single dielectric dispersions within wide frequency ranges but, at lower frequencies, the dielectric constant follows either Curve A or B. The temperature-dependence of f_m satisfies the relation

$$f_m = f_{mo} \exp(-H/kT) \quad (3)$$

where f_{mo} is the pre-exponential factor. It has been confirmed by many workers for a number of glass compositions that the activation energy values for d.c. conduction and for single dielectric dispersion are the same, as illustrated in Fig. 3 [16]. There is some controversy on this subject, and this will be discussed later.

The TSPC/TSDC measurements are obtained as follows (Fig. 4). The sample is cooled to T_0, biased by d.c. field E_p, heated to an appropriate temperature, and the current induced by build-up of polarization as well as by conduction is measured as TSPC. Independently, or immediately after the TSPC run as in Fig. 4, the sample is polarized at a given temperature T_p, quenched to T_0 with the field still applied, and heated without field, and we observe TSDC by the relaxation of frozen-in polarization. Both TSPC and TSDC should give peaks of identical magnitude at an identical temperature when their origins are the same.

0022–2461/87 $03.00 + .12

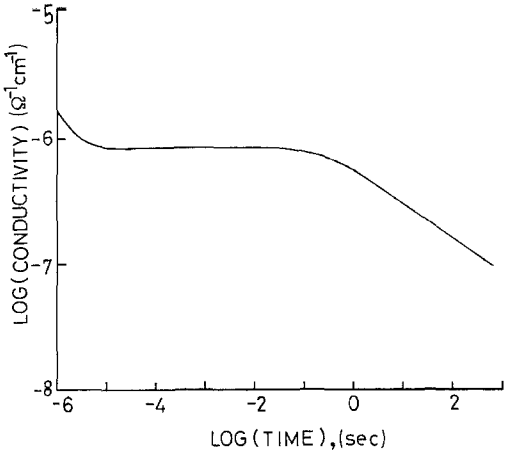

Figure 1 Electrical conductivity of $30Li_2O \cdot 70SiO_2$ glass as a function of time, measured at 80° C [15].

2. Charge carriers

When alkali (R_2O) is added to the silica glass, some Si–O–Si bonds are broken and nonbridging oxygen ions are generated (Fig. 5). The ionic species as alkali and nonbridging oxygen are distributed among the strongly covalent network or chain structure of Si–O, Ge–O, B–O or P–O. Therefore, those ionic species may be mobile and become the charge carriers for conduction. It is now well known that various monovalent and multivalent cations can conduct or be injected into glass by ion-exchange, glow discharge or ion-implantation. In addition to cations, anions such as nonbridging oxygen, can conduct to the anode. For glasses containing large amounts of transition metals, it is believed that conduction proceeds by electronic or polaronic hopping between different charge states of transition metals.

3. Conduction polarization of alkali ions

Various alkali-containing silicate [1–4, 6–8, 10–14, 17–21], germanate [5] and phosphate [9, 22] glasses show a TSPC/TSDC peak, P1, in the low-temperature region with a peak height of 10^{-13} to $10^{-15}\Omega^{-1}$cm^{-1} (Fig. 6). We assigned the peak as arising from conduction polarization of alkali ions, as discussed below.

In the glassy materials where ample spaces are

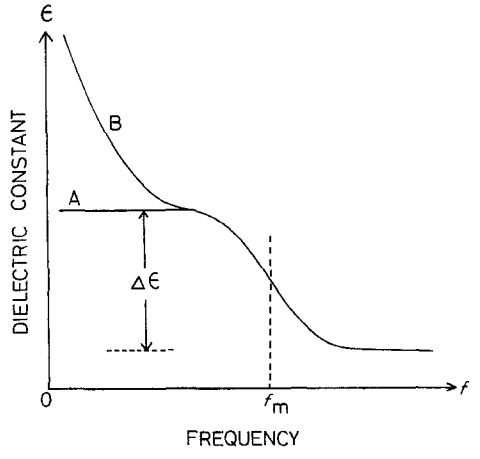

Figure 2 Dielectric constant of oxide glass as a function of frequency, illustrating a dispersion at f_m with magnitude $\Delta\varepsilon$ and another dispersion at lower frequencies (Curve B). Curve A is found for some glasses.

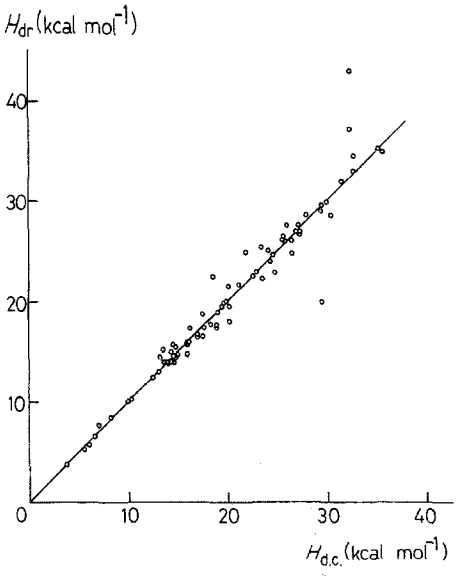

Figure 3 Comparison of activation energies for d.c. conduction ($H_{d.c.}$) and for dielectric relaxation (H_{DR}) of various oxide glasses [16].

provided by its disordered structure, each jump of the charge carriers for conduction can be treated as independent of each other. This is substantiated by the fact that, in the glass, the observed electrical conductivity satisfies, at least qualitatively, theoretical description [23]

$$\sigma_{d.c.} = \frac{ne^2\lambda^2\nu_0}{\alpha kT}\exp(-H/kT) \qquad (4)$$

based on the independent-jump hypothesis, where n is the charge carrier density, λ the average jump distance, α the number of possible jump directions, and ν_0 the oscillation frequency of the charge carriers which is given as the pre-exponential factor of the jumping frequency

$$\nu = \nu_0 \exp(-H/kT) \qquad (5)$$

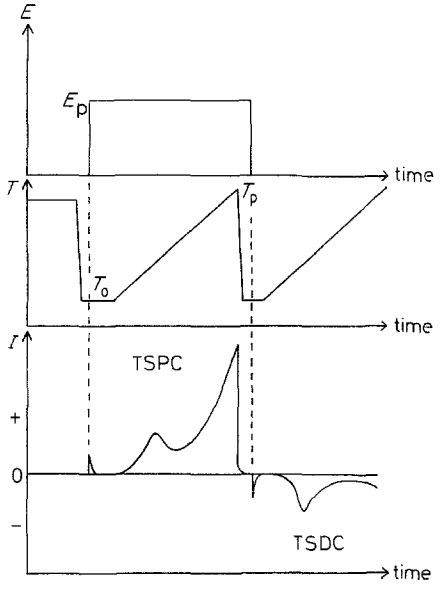

Figure 4 Experimental procedure for TSPC/TSDC measurements, where applied field, E, temperature, T, and the induced current, I, are shown as a function of time.

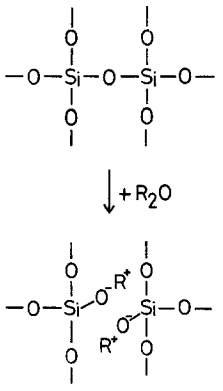

Figure 5 Addition alkali (R_2O) to silica glass breaks some of the Si–O–Si bonds and generates nonbridging oxygen ions.

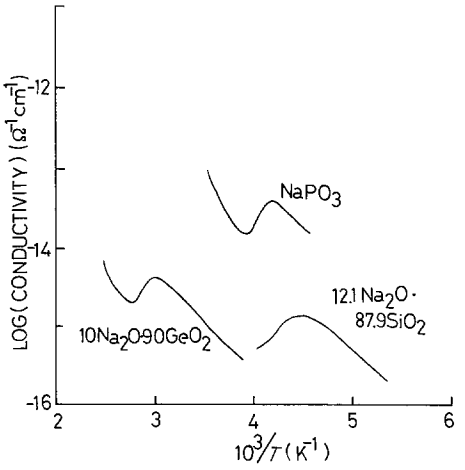

Figure 6 P1 peaks of several sodium-containing oxide glasses [11].

out of the potential well surrounded by an energy barrier H.

The probability distribution of jump directions or resultant microscopic distribution of the charge carriers must be distorted from its original symmetry when the sample is biased by an applied field (Fig. 7). Assuming an independent-jump hypothesis, each jump of the charge carriers for conduction generates polarization, independently and perpetually. As a whole, the generation process of microscopically distorted distribution of the charge carriers gives rise to the TSPC peak, while the opposite process applies to the TSDC peak. We term the polarization caused by such an elementary process of conduction the "conduction polarization" [5]. The conduction polarization model requires that the relevant TSPC/TSDC peak temperature, T_{km}, must be related to the activation energy for conduction, H, by

$$\frac{H}{kT_m^2} = \frac{\nu_0}{\beta} \exp\left(-\frac{H}{kT_m}\right) \tag{6}$$

where β is the heating rate. Since the values of ν_0 are known for some glasses [24–27] and are expected to change little with alkali content [25], we estimated H from Equation 6 using observed P1 peak temperatures (Table I). The agreement is good, in view of the scatter of reported activation energy values.

Any relaxation process can be characterized by the relaxation time, τ, defined by

$$\tau = \tau_0 \exp(H/kT) \tag{7}$$

where τ_0 is the pre-exponential factor. Suppose τ is the time spanned by a single jump of the charge carriers, the magnitude of dielectric dispersion $\Delta\varepsilon$ divided by τ should give d.c. conductivity from

$$\frac{\Delta\varepsilon}{\tau} = \left(\frac{\Delta Q}{\tau E_p}\right)\frac{1}{\varepsilon_0} = \frac{\sigma_{d.c.}}{\varepsilon_0} \tag{8}$$

provided each jump for conduction generates conduction polarization, because $\sigma_{d.c.}$ is equal to the flow rate of the charge carriers into the electrode per unit applied field, where ε_0 is the permittivity of free space and ΔQ is the difference in total electron density on a given electrode at frequencies below and above the relevant dispersion at which

$$2\pi f_m \tau = 1 \tag{9}$$

From Equations 8 and 9 we obtain the well-known relation between electrical conduction and dielectric relaxation [9, 14, 28]

$$\sigma_{d.c.} = \varepsilon_0 \Delta\varepsilon 2\pi f_m \tag{10}$$

TABLE I Activation energies for conduction, as determined from Equation 6 using observed P1 peak temperatures, in addition to TSPC slopes and reported activation energy values [3, 9, 12, 13]. Also listed are calculated activation energies for conduction of nonbridging oxygen ions in ADR using observed P2-peak temperatures [8, 12]

Glass composition	Calculated activation energies from P1 peak temperatures (kcal mol^{-1})	Calculated activation energies from P2 peak temperatures (kcal mol^{-1})	TSPC slopes (kcal mol^{-1})	Reported activation energies for conduction (kcal mol^{-1})
$Li_2O \cdot 2SiO_2$	14.8 ± 0.4	19.2	15.6 ± 0.8	14.6–14.9
$Na_2O \cdot 2SiO_2$	15.6 ± 0.4	20.1	15.7 ± 1.1	14.0–15.0
Commercially available soda lime	18.2	23.4	18.4 ± 0.8	19.1–23.5
Pyrex	20.2	26.0	21.1 ± 0.9	18.4–22.4
$10Na_2O \cdot 90GeO_2$	22.9		21.3	23.4–24.5
$27.5Na_2O \cdot 72.5GeO_2$	15.5		16.0	15.9
$NaPO_3$	16.0 ± 0.1		16.2 ± 0.2	14.5–17.9
$30PbO \cdot 70SiO_2$	28.3		28.4	28.3–31.1
$35PbO \cdot 65SiO_2$	26.5		27.0	27.5–28.7
$40PbO \cdot 60SiO_2$	26.0		26.5	26.5–29.1
$45PbO \cdot 55SiO_2$	24.1		25.1	24.1–27.0
$50PbO \cdot 50SiO_2$	24.4		25.1	24.1–27.0

TABLE II Magnitude of polarization $\Delta\varepsilon$ for glasses of similar composition, as determined from dielectric relaxation and from TSDC [5]

Composition (mol %)	$\Delta\varepsilon$ (dielectric loss)	Composition (mol %)	$\Delta\varepsilon$ (TSDC)
$15Na_2O \cdot 85SiO_2$	16	$14.6Na_2O \cdot 85.4SiO_2$	14.1
$30Na_2O \cdot 70SiO_2$	27	$25Na_2O \cdot 75SiO_2$	25.5
$15Na_2O \cdot 85B_2O_3$	9.2	$16Na_2O \cdot 84B_2O_3$	14.9
$16Na_2O \cdot 74B_2O_3 \cdot 10SiO_2$	7.5	$14.7Na_2O \cdot 68.9B_2O_3 \cdot 16.4SiO_2$	16.6
$10Na_2O \cdot 25B_2O_3 \cdot 65SiO_2$	17	$11.7Na_2O \cdot 15.1B_2O_3 \cdot 73.2SiO_2$	21.2
$16Na_2O \cdot 10CaO \cdot 74SiO_2$	27	$15Na_2O \cdot 10CaO \cdot 75SiO_2$	26.0
$3Na_2O \cdot 97GeO_2$	17.5	$2Na_2O \cdot 98GeO_2$	28.1

which is found to hold for various oxide glasses (Fig. 8) [16, 29].

The inverse also holds true. According to the conduction polarization model [5], the magnitude of conduction polarization, P, is given by

$$\frac{P}{E_p} = \frac{ne^2\lambda^2}{\alpha kT} = \varepsilon_0\Delta\varepsilon \quad (11)$$

Table II shows comparison of the magnitude of polarization, $\Delta\varepsilon$, for glasses of similar composition as determined from dielectric relaxation and from Equation 11 using observed P1 peaks [5]. We obtain from

$$\sigma_0 = \frac{ne^2\lambda^2\nu_0}{\alpha kT} = \varepsilon_o\Delta\varepsilon 2\pi f_{mo} = \frac{ne^2\lambda^2}{\alpha kT} 2\pi f_{mo} \quad (12)$$

the relation

$$\nu_0 = 2\pi f_{mo} \quad (13)$$

hence, from Equations 9 and 5

$$\tau = \frac{1}{2\pi f_m} = \frac{1}{\nu_0 \exp(-H/kT)} = \frac{1}{\nu} \quad (14)$$

that is, τ must be equal to the time spanned by the charge carriers to do single jumps.

From Equation 6 we can plot the values of H as a function of T_m (Fig. 9) and the values of ν at P1 peak maximum as a function of $1/T_m$ (Fig. 10) for some oxide glasses studied so far [14]. For convenience sake, β is fixed at 0.10 deg sec^{-1}. In spite of variance of ν_0 by a factor of 3, the estimated values of H and $\nu(T_m(P1))$ are on the straight lines passing through the origin. It is reasonable to have average jumping frequencies around 1×10^{-2} Hz at P1 peak maxima because the conduction polarization model requires that, at the end temperature of the P1 peak, the mobile charge carriers should finish their conductive jumps at least once. It is also reasonable to observe motional narrowing of the lithium NMR line in $Li_2O \cdot 2SiO_2$ glass at 300 K [30] because, at this temperature, the jumping frequency of lithium ions is 10^2 Hz which seems to be sufficient for smearing out the h.f. structure.

From Equations 1, 3, 10 and 11 we obtain the relation

$$\frac{f_{mo}}{\sigma_0} = \frac{1}{2\pi\varepsilon_0\Delta\varepsilon} = \frac{E_p}{2\pi P} \quad (15)$$

which suggests that the ratio of the pre-exponential factors for $\sigma_{d.c.}$ and f_m can be determined from the area covered by the P1 peak. In truth the estimated values of the ratio f_{mo}/σ_0 from the P1 peaks of several oxide glasses (Table III) [12] agree well with those derived from separate measurements of conduction and dielectric relaxation (Fig. 11) [16].

From the above discussion we conclude that the P1 peak is in one-to-one correspondence with single dielectric dispersion observed for all the glasses studied so far and arises from an elementary process of conduction as conduction polarization. Although there is an opposing opinion [1, 18–22] that orientational polarization of alkali–nonbridging oxygen dipoles would be responsible for the P1 peak, it fails because of an abnormally large dipole distance found for some sodium germanate glasses [5] and the lack of observation of relevant dielectric dispersion due to dipolar orientation.

4. Conduction polarization of nonbridging oxygen ions

Three TSPC/TSDC peaks, P1, P2 and P3, were found within the temperature range 77 to 700 K for alkali

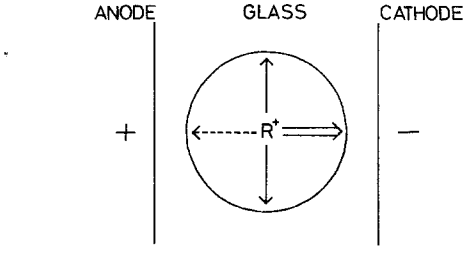

Figure 7 Origin of conduction polarization of a charge carrier (R^+) in the electric field, showing distortion of probability distribution of jump directions to the cathode side, rather than to the anode side.

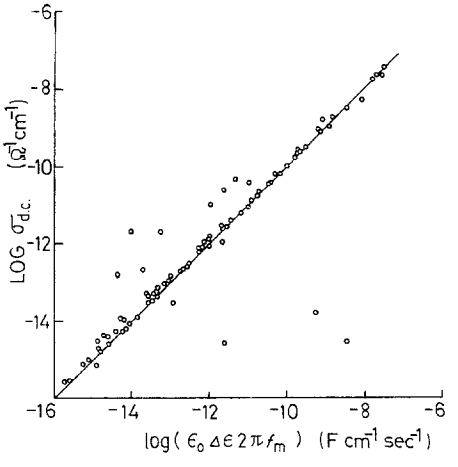

Figure 8 Comparison of d.c. conductivities with $\varepsilon_0\Delta\varepsilon 2\pi f_m$ for various oxide glasses [16].

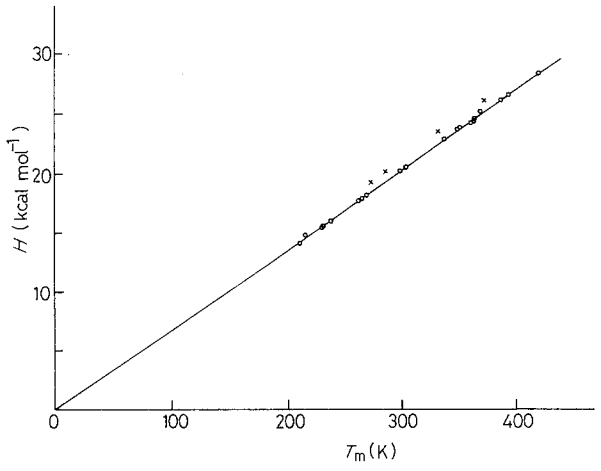

Figure 9 Calculated activation energies for conduction from Equation 6 using the temperatures T_m at (○) P1 or (x) P2 peak maxima for some oxide glasses [14].

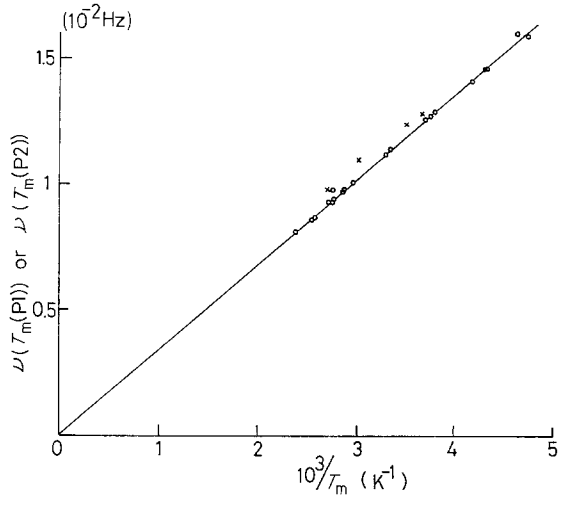

Figure 10 Calculated jumping frequencies at (○) P1 or (x) P2 peak maxima from Equations 5 and 6 as a function of reciprocal T_m [14].

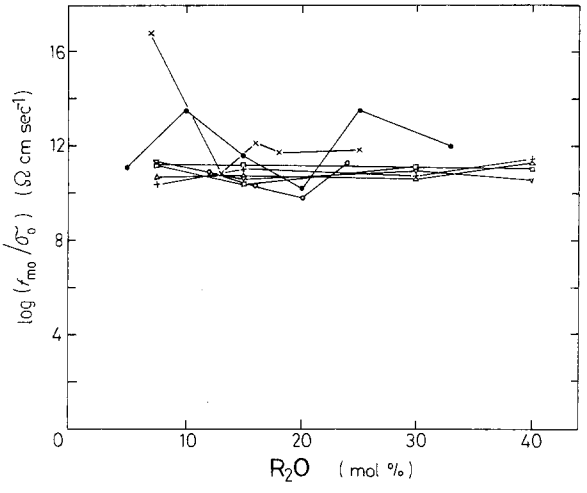

Figure 11 Ratio of pre-exponential factors for dielectric dispersion frequency, f_m, and for d.c. conductivity, $\sigma_{d.c.}$, as a function of alkali content for some glass systems: (□) xLi$_2$O · (100 − x)SiO$_2$, (△) xNa$_2$O · (100 − x)SiO$_2$, (▽) xK$_2$O · (100 − x)SiO$_2$, (+) xRb$_2$O · (100 − x)SiO$_2$, (○) xNa$_2$O · 10CaO · (90 − x)SiO$_2$, (●) xNa$_2$O · (100 − x)B$_2$O$_3$, and x for xNa$_2$O · 10SiO$_2$ · (90 − x)B$_2$O$_3$ [12, 16].

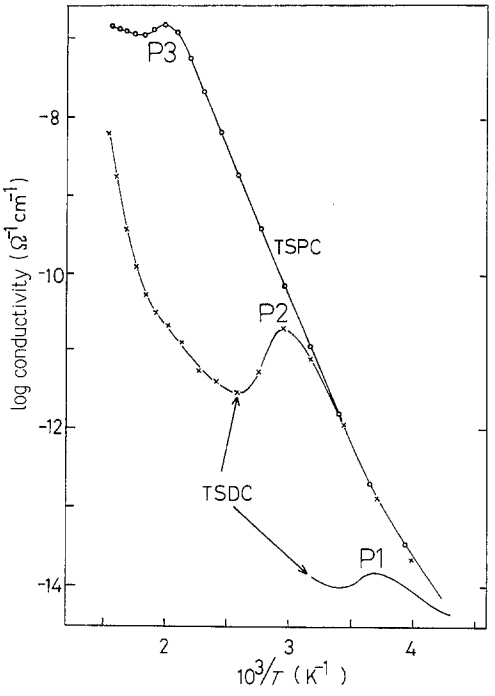

Figure 12 Typical TSPC/TSDC curves for commercially available soda-lime glass, showing P1, P2 and P3 peaks in the order of increasing temperatures [12].

silicate glasses (Fig 12). In the TSPC curve the P1 and P2 peaks are hidden by an overwhelming current of the P3 peak, but are found in the TSDC curves. However, even in the TSDC run, the P1 peak emerges out of the overlapping current of the P2 peak only when the sample is polarized at temperatures as low as possible. For glasses other than alkali silicate there is no sign of the presence of the P2 peak for the TSPC/TSDC runs up to 500 K.

Since alkali ions are the dominant charge carriers in alkali silicate glass, alkali ions will first conduct to the cathode and generate the alkali-depleted region (ADR) near the anode (Fig. 13). Alkali accumulation near the cathode and depletion near the anode was verified directly by means of the secondary-ion mass spectroscopy (Fig. 14) [10]. As alkali depletion proceeds, the effective field within ADR will develop to the level where nonbridging oxygen ions which are not charge-compensated can move to the anode. Oxygen movement to the anode has already been demonstrated by several techniques [31–33]. It is reasonable then to expect that the P2 peak would arise from conduction polarization of nonbridging oxygen ions in ADR. One piece of supporting evidence is the disappearance of the P2 peak when silver instead of

TABLE III Ratios f_{mo}/σ_0 and $n\lambda^2/N\lambda_{av}^2$ for several alkali silicate glasses, as determined from the areas covered by the P1 peaks [12]

Glass composition	f_{mo}/σ_0 (Ω cm sec^{-1})	$n\lambda^2/N\lambda_{av}^2$
Pyrex	7.5×10^{10}	0.14
Commercially available soda-lime	3.0×10^{10}	0.22
R$_2$O · 3SiO$_2$ (R = Li, Na, K, Rb)	(7.0 to 13.2) × 10^{10}	0.043–0.048

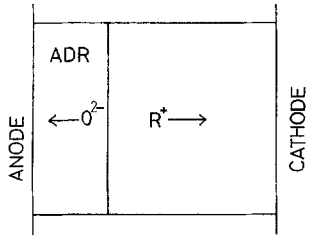

Figure 13 Formation of alkali-depleted region (ADR) near the anode as alkali conduction to the cathode proceeds. In ADR the movement of nonbridging oxygen ions to the anode takes place.

gold was used as the anode [8], for silver can easily be injected into glass and hinder the conductive motion of nonbridging oxygen ions in ADR by charge-compensation and/or steric hindrance (Fig. 15).

In the discussion above we refer to samples as thick as ~ 1 mm. When blown glass films of several micrometres in thickness were used instead, the electrical conductivity was reduced to several hundredths [6, 8] due, possibly, to the formation of some dielectric layer [11]. By such a drastic reduction in electrical conductivity, or the P3 peak, we can observe the P2 peak even in the TSPC run (Fig. 16) [6]. From the coincidence of the position and magnitude of the P2 peak for both TSPC and TSDC runs, it is evident that the P2 peak arises from electric polarization. By the same reasoning the P3 peak was found not to be due to polarization because of the absence of the corresponding peak in the TSDC curve.

The infrared measurements of alkali silicate glasses show a shift of the Si–O–Si antisymmetric stretching band of the silica glass at $\sim 1100\,cm^{-1}$ to lower frequencies and its splitting into two by the formation of nonbridging oxygen ions as the alkali content increases [34, 35]. If the value of $1000\,cm^{-1}$ is adopted as equal to ν_0 for nonbridging oxygen ions in our glass, Equation 6 gives the calculated activation energies for conduction of nonbridging oxygen ions in ADR as roughly 4 to 6 kcal mol^{-1} larger than that for alkali ions [8] (Table I). It should be noticed that those values are

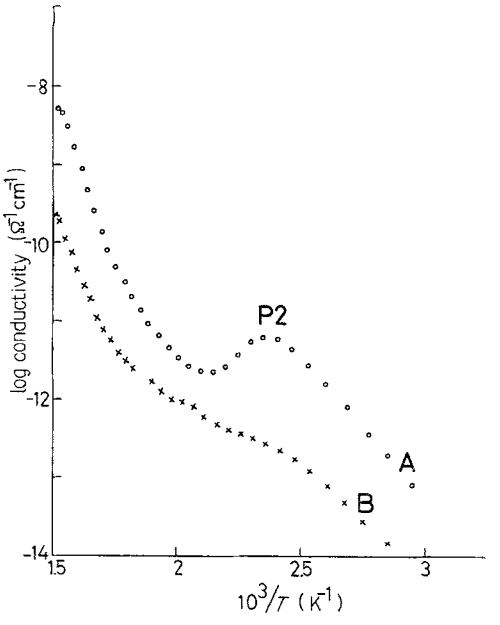

Figure 15 TSDC curves of pyrex glass samples with gold anode (Curve A) or with silver anode (Curve B), measured immediately after TSPC runs up to 700 K with $200\,V\,cm^{-1}$.

for conduction in ADR, not for conduction in the bulk where the movement of nonbridging oxygen ions is almost improbable. From the magnitude of polarization for P2, the effective field in ADR is estimated to be several hundreds to thousands times larger than the applied field. Further evidence in favour of our assignment comes from the fact that the jumping frequency at P2 peak maximum, $\nu(T_m(P2))$, is around $\sim 1 \times 10^{-2}$ Hz, just the same as for the P1 peak (Fig. 10).

The magnitude of polarization, $\Delta\varepsilon$, for the P2 peak is calculated from Equation 11 to be $\sim 10^4$ for various alkali silicate glasses [12]. The dielectric measurements of alkali silicate glass show two major dispersions, one which is connected with P1 and another found at lower frequencies (Curve B, Fig. 2). Since the latter dispersion (termed electrode polarization [36]) levels

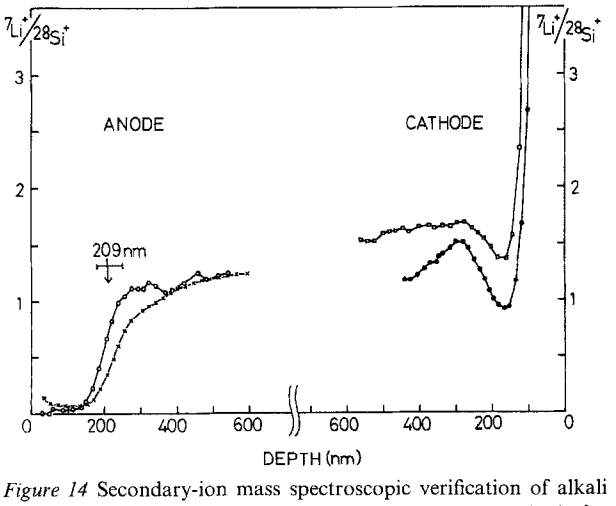

Figure 14 Secondary-ion mass spectroscopic verification of alkali depletion near the anode and accumulation near the cathode for polarized $Li_2O \cdot 2SiO_2$ glass sample. Estimated ADR width, on the assumption that the current flowed in the external circuit during polarization is carried solely by lithium ions in ADR, is 208.8 nm [10].

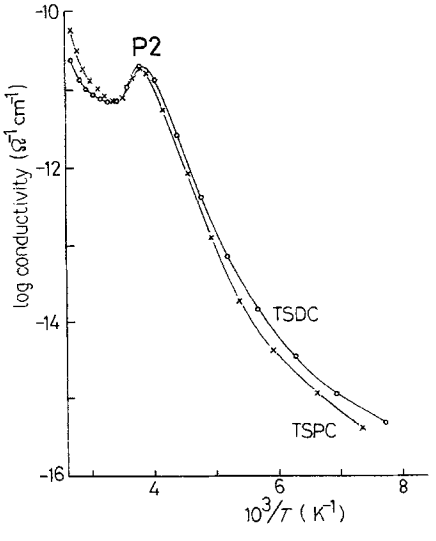

Figure 16 TSPC/TSDC curves of $Li_2O \cdot 2SiO_2$ glass sample, 8 μm thick, where E_p is $1.2\,kV\,cm^{-1}$ [6]. Owing to large reduction of the P3 peak, the P2 peak appeared even in the TSPC curve.

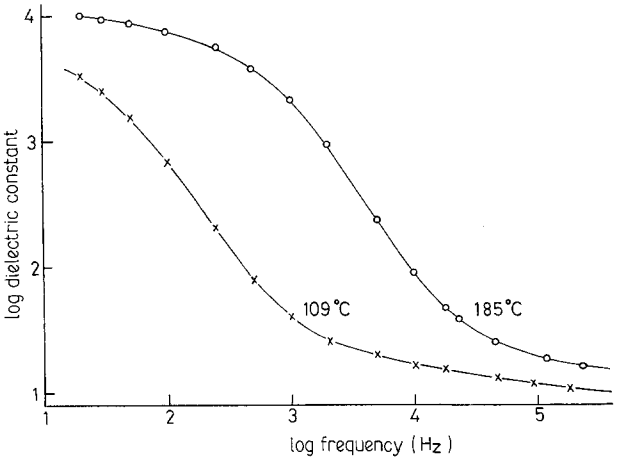

Figure 17 Dielectric constant of $Na_2O \cdot 3SiO_2$ glass, measured at 185 and 109° C [37].

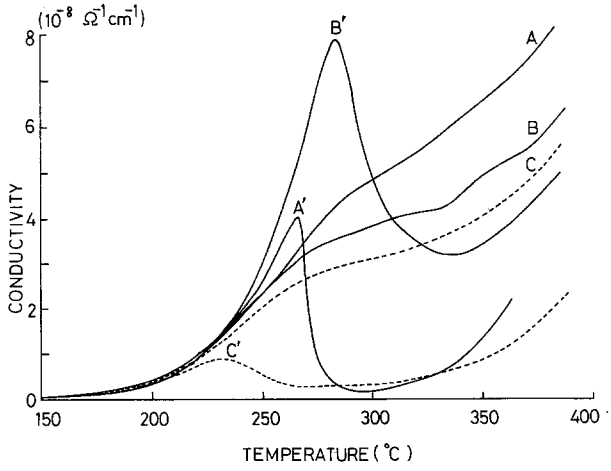

Figure 19 TSPC curves for three previously unpolarized samples of pyrex glass, where E_p is 200 V cm^{-1}. The second TSPC runs (A′, B′, C′) were made the next day after the first runs (A, B, C) were done, with the same polarity. Corresponding TSDC curves are not shown for clarity [12].

off at $\sim 10^4$ [37] (Fig. 17), it is reasonable to assign the lower-frequency dispersion as due to the P2 peak. The absence of this dispersion in, for example, electron-hopping glasses as $55FeO_x \cdot 45P_2O_5$ [38] is in accordance with our assignment. A scatter in the lower-frequency dispersion for samples with different surface conditions [37] may arise from the different feasibility of ADR formation.

5. Conduction polarization of divalent cations

There is controversy concerning whether or not divalent or higher-valent cations can be the charge carriers for conduction. For lead silicate glass some papers [13] claim that the dominant charge carriers would be the Pb^{2+} ions, the protons due to water ingredient, the impurity alkali ions or the electrons. From analysis of single TSDC peaks found for xPbO · (100 − x)SiO_2 glasses with $30 \leqslant x \leqslant 50$ [39] (Table I), it was concluded [13] that the Pb^{2+} ions would be responsible for observed conduction.

Similarly, the single TSPC peaks found for 67.5 and 62.5 mol % CdO-containing borosilicate glasses [40] are analysed from Equations 5 and 6 [14]. Because of the presence of electronic as well as photoconductivity

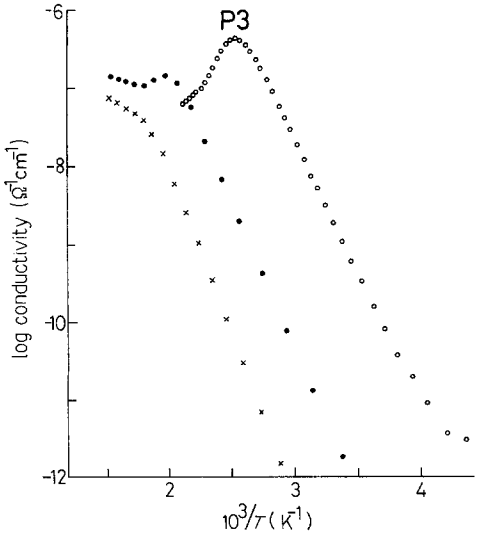

Figure 18 TSPC curves of previously unpolarized $Li_2O \cdot 2SiO_2$ (○), commercially available soda-lime (●) and pyrex (x) glasses [10, 12].

for those glasses [40, 41], a comparison of the calculated and observed activation energy values as in Table I fails. However, since the calculated jumping frequencies at TSPC peak maximum lie at $\sim 1 \times 10^{-2}$ Hz as for the conduction polarization peaks of alkali, nonbridging oxygen and Pb^{2+} ions (Fig. 10), those peaks may be due to conduction polarization of the Cd^{2+} ions.

6. Heterogeneous distribution of charge carriers

When Equation 11 is applied to the P1 peak, n, λ and α are still unknown. Assuming a homogeneous distribution of the charge carriers with nominal density N, $\alpha = 6$, and the average jump distance, λ_{av}, as equal to the separation between two nearest-neighbour charge carriers, λ_{av} is given by

$$\lambda_{av} = \left(\frac{6}{\pi N}\right)^{1/3} \tag{16}$$

whence the ratio $n\lambda^2/N\lambda_{av}^2$ can be a measure of the fraction of overall charge carriers which contribute to conduction, or to the conduction polarization peak P1. The right column of Table III gives the estimated values of the ratio for several oxide glasses. As is generally believed, only a small fraction of overall alkali ions contributes to conduction.

The slope and magnitude of the TSPC conductivity up to P3 peak maximum agrees well with those for reported d.c. conductivity [42] (Table I), which means that the space-charge effect can be overcome by an exponentially growing conduction current up to the P3 peak temperature. Around this temperature, however, the potential drop at ADR becomes so noticeable as to reduce an effective field in the glass bulk, hence we observe the P3 peak.

Fig. 18 shows a comparison of the TSPC curves of several previously unpolarized alkali silicate glasses. As is apparent, the sharpness of the P3 peak becomes lessened with decreasing alkali content to a complete absence for the pyrex glass. Nevertheless, even for the pyrex glass, the P3 peak revealed itself in subsequent TSPC runs made after an initial TSPC/TSDC cycle

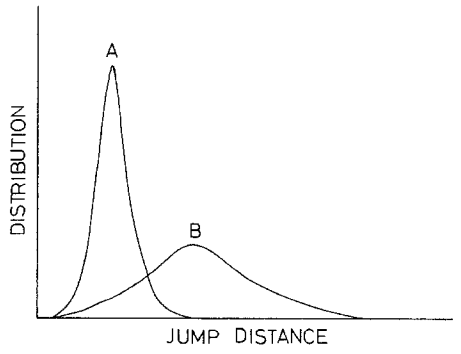

Figure 20 A schematic drawing showing how the distribution function of jump distance changes with decreasing alkali content from A to B.

(Fig. 19). As stated above, the P3 peak arises by a slowing down of the conduction current by the development of highly resistive ADR near the anode. Therefore, ADR must be generated within as narrow a temperature range as possible in order for the P3 peak to appear. As alkali content decreases from A to B (Fig. 20), the distribution function of jump distance becomes wider, as would the necessary temperature ranges for depleting overall mobile carriers from ADR. This may be the reason for the absence of the apparent P3 peak for previously unpolarized pyrex glass [13].

Once the sample is polarized, structural rearrangement would take place in the ADR as infrared absorption spectra suggested [31], where a silica-like structure was found. Such a structural change would permit the P3 peak to appear in the subsequent TSPC runs by allowing back-diffused alkali ions in ADR to move more easily. It must be noted here that, in the TSDC run, the TSDC current other than the P1 and P2 peaks arises by back-diffusion of alkali ions into ADR [10]. It is also suggested [12] that the alkali-accumulated region near the cathode suffers similar structural change during an initial TSPC run. Furthermore, a scatter of the position and magnitude of the P3 peak from sample to sample, as shown in Fig. 19, would reflect a heterogeneous nature of the glass structure, because the relevant phenomenon is restricted to within a very narrow section of less than several micrometres in thickness from the anode so that averaging as in the bulk cannot be achieved.

7. Conduction and neutralization

As we know, the conduction process refers to the impingement of the charge carriers into the electrode. For electrolysis of liquid electrolyte, Faraday's law holds, saying that the amount of electrolytically deposited material is equal to the total charge which flowed in the external circuit, or that electrical conduction is followed by neutralization of relevant charge carriers at the electrode. However, this common sense fails in the discussion of the conduction process in solid electrolyte where, due to its very low conductivity, it is believed that some of the charge carriers which reach the electrode cannot be neutralized and remain as a space charge [31, 43, 44].

When teflon films, several tens of micrometres

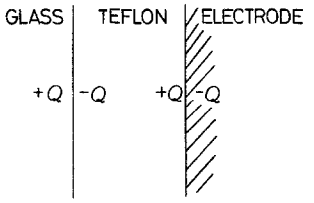

Figure 21 Charge balance at glass/teflon/electrode interfaces which is required for maintaining local charge neutrality.

thick, were inserted between the electrodes and the glass, the conduction current was drastically reduced and only the P1 peak remained in the TSPC curves of several alkali-containing oxide glasses [21, 22]. As the magnitude of the P1 peak changed little, this phenomenon is not due to reduction of the applied field by the presence of the films. When the charge, $+Q$, is accumulated on the glass surface, $-Q$ must be on the adjacent teflon surface in order to maintain local charge neutrality at the interface (Fig. 21). Teflon is a non-polar polymer but can be polarized by conduction polarization etc. [45]. Since conduction is made up of sequential jumps of mobile alkali ions, the absence of the conduction current means that alkali ions, which by single conductive jumps reach the glass–teflon interface and give the conduction polarization peak P1 by induction, cannot be neutralized there, and retard the following alkali ions to come to the interface by coulombic repulsion. That is, this experiment demonstrates that conduction should be accompanied by neutralization of the incoming charge carriers into the electrode in order for conduction to take place. Therefore, alkalis which accumulate near the cathode must be neutral, as colloids [31, 32] etc. The presence of a noticeable potential drop near the cathode in an early stage of biasing [44] (Fig. 22) may then be due not to unneutralized charge carriers

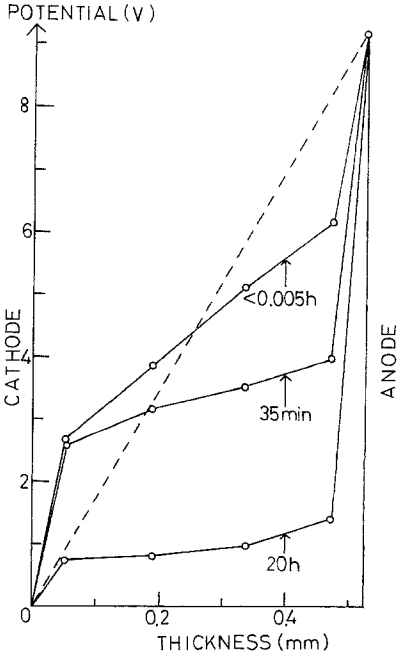

Figure 22 Potential probe experiments of alkali lead silicate glass sample, 0.52 mm thick, measured at three different times after application of 9.2 V [44].

but to other interfacial phenomena such as impurity adsorption and/or chemical modification of the surface.

The above statement is a matter of course if we refer to one of Maxwell's equations

$$\text{rot } H = i + \frac{\partial D}{\partial t} \tag{17}$$

where H is the magnetic field, i the current due to conduction and D the displacement. Equation 17 means that the charge carrier motion in any medium can be described by the sum of contributions from the charge transfer process at the medium-electrode or -vacuum interface (to give the conduction current i) and from the charge accumulation/depletion process at the interface (to give the displacement current $\partial D/\partial t$). Both processes are mutually complementary and should not be confused.

References

1. A. DOI, *J. Appl. Phys.* **50**, (1979) 1291.
2. *Idem, Jpn J. Appl. Phys.* **19** (1980) 2085.
3. A. DOI and D. E. DAY, *J. Mater. Sci.* **15** (1980) 3047.
4. A. DOI, *ibid.* **16** (1981) 2028.
5. A. DOI and D. E. DAY, *J. Appl. Phys.* **52** (1981) 3433.
6. A. DOI, *J. Mater. Sci.* **17** (1982) 2087.
7. *Idem, Jpn J. Appl. Phys.* **21** (1982) 987.
8. *Idem, ibid.* **22** (1983) 228.
9. *Idem, J. Mater. Sci. Lett.* **3** (1984) 613.
10. A. DOI, T. MIWA and A. MIZUIKE, *J. Mater. Sci.* **20** (1985) 1787.
11. A. DOI, *J. Mater. Sci. Lett.* **4** (1985) 985.
12. A. DOI and S. MARUNO, *J. Mater. Sci.* **21** (1986) 1863.
13. A. DOI, *J. Mater. Sci. Lett.* **5** (1986) 443.
14. *Idem, ibid.* **5** (1986) 635.
15. D. L. KINSER and L. L. HENCH, *J. Amer. Ceram. Soc.* **52** (1969) 638.
16. H. NAMIKAWA, *J. Non-Cryst. Solids* **18** (1975) 173.
17. R. M. CATCHINGS, *J. Appl. Phys.* **50** (1979) 2813.
18. C. M. HONG and D. E. DAY, *J. Mater. Sci.* **14** (1979) 2493.
19. *Idem, J. Amer. Ceram. Soc.* **64** (1981) 61.
20. H. D. JANNEK and D. E. DAY, *ibid.* **64** (1981) 227.
21. A. K. AGARWAL and D. E. DAY, *ibid.* **65** (1982) 111.
22. M. B. DUTT and D. E. DAY, *J. Non-Cryst. Solids* **71** (1985) 125.
23. A. E. OWEN, in "Progress in Ceramic Science Vol. 3", edited by J. E. Burke (Pergamon, New York, 1963) p. 84 .
24. G. J. EXARHOS and W. M. RISEN Jr, *Solid State Commun.* **11** (1972) 755.
25. G. J. EXARHOS, P. J. MILLER and W. M. RISEN, Jr, *J. Chem. Phys.* **60** (1974) 4145.
26. C. A. WORRELL and T. HENSHALL, *J. Non-Cryst. Solids* **29** (1978) 283.
27. T. FURUKAWA, S. A. BRAWER and W. B. WHITE, *J. Mater. Sci.* **13** (1978) 266.
28. A. DOI, *J. Non-Cryst. Solids* **29** (1978) 131.
29. T. NAKAJIMA, Conference on Electrical Insulation and Dielectric Phenomena, Williamsburg (1971).
30. J. R. HENDRICKSON and P. J. BRAY, *J. Chem. Phys.* **61** (1974) 2754.
31. D. E. CARLSON, K. W. HANG and G. F. STOCKDALE, *J. Amer. Ceram. Soc.* **55** (1972) 295.
32. *Idem, ibid.* **55** (1972) 337.
33. K. TAKIZAWA, *ibid.* **61** (1978) 475.
34. R. HANNA and G-J. SU, *ibid.* **47** (1964) 597.
35. N. NEUROTH, *Glastech. Ber.* **41** (1968) 243.
36. M. TOMOZAWA, in "Treatise on Materials Science and Technology", Vol. 12, edited by M. Tomozawa and R. Doremus (Academic, New York, 1977) p. 283.
37. C. KIM and M. TOMOZAWA, *J. Amer. Ceram. Soc.* **59** (1976) 127.
38. K. W. HANSEN and M. T. SPLANN, *J. Electrochem. Soc.* **113** (1966) 895.
39. C. M. HONG, D. E. DAY, R. A. WEEKS and D. L. KINSER, *J. Non-Cryst. Solids* **46** (1981) 389.
40. L. J. MANFREDO and L. D. PYE, *J. Appl. Phys.* **49** (1978) 682.
41. D. W. STRICKLER and R. ROY, *J. Mater. Sci.* **6** (1971) 200.
42. C. M. HONG and D. E. DAY, *J. Appl. Phys.* **50** (1979) 5352.
43. P. M. SUTTON, *J. Amer. Ceram. Soc.* **47** (1964) 188.
44. *Idem, ibid.* **47** (1964) 219.
45. A. DOI, *J. Appl. Phys.* **59** (1986) 2068.

Received 27 May
and accepted 18 August 1986